

Reactions of a Chromium(III)-Superoxo Complex and Nitric Oxide That Lead to the Formation of Chromium(IV)-Oxo and Chromium(III)-Nitrito Complexes

Atsutoshi Yokoyama,[†] Kyung-Bin Cho,[†] Kenneth D. Karlin,^{*,†,‡} and Wonwoo Nam^{*,†}

[†]Department of Bioinspired Science and Department of Chemistry and Nano Science, Ewha Womans University, Seoul 120-750, Korea

[‡]Department of Chemistry, The Johns Hopkins University, Baltimore, Maryland 21218, United States

S Supporting Information

ABSTRACT: The reaction of an end-on Cr(III)-superoxo complex bearing a 14-membered tetraazamacrocyclic TMC ligand, $[\text{Cr}^{\text{III}}(14\text{-TMC})(\text{O}_2)(\text{Cl})]^+$, with nitric oxide (NO) resulted in the generation of a stable Cr(IV)-oxo species, $[\text{Cr}^{\text{IV}}(14\text{-TMC})(\text{O})(\text{Cl})]^+$, via the formation of a Cr(III)-peroxynitrite intermediate and homolytic O–O bond cleavage of the peroxynitrite ligand. Evidence for the latter comes from electron paramagnetic resonance spectroscopy, computational chemistry and the observation of phenol nitration chemistry. The Cr(IV)-oxo complex does not react with nitrogen dioxide (NO_2), but reacts with NO to afford a Cr(III)-nitrito complex, $[\text{Cr}^{\text{III}}(14\text{-TMC})(\text{NO}_2)(\text{Cl})]^+$. The Cr(IV)-oxo and Cr(III)-nitrito complexes were also characterized spectroscopically and/or structurally.

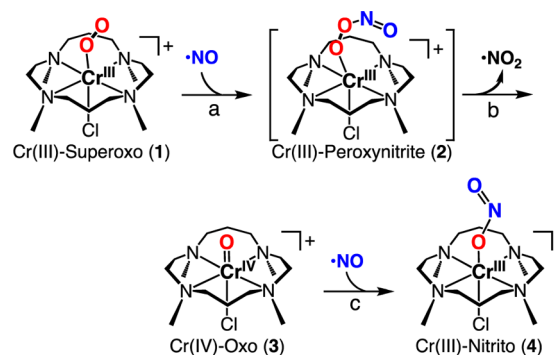
Nitric oxide (NO) is a ubiquitous signal transduction molecule found in a wide variety of physiological processes, such as in cellular signaling leading to smooth muscle vasodilation, platelet disaggregation, and neurotransmission and in the immune response to bacterial infection.¹ However, NO itself is a toxin because of the reactivity derived from its radical character and ability to form more reactive and deleterious oxidation products, such as nitrogen dioxide (NO_2) and peroxynitrite (PN, oxoperoxonitrate(-), $^-\text{OON}=\text{O}$), in the presence of transition metals.² In this context, various life forms have constructed detoxification systems: widely occurring nitric oxide dioxygenases (NODs) are enzymes that catalyze the conversion of toxic NO to biologically atoxic nitrate (NO_3^-) with NAD(P)H (i.e., $2\text{NO} + 2\text{O}_2 + \text{NAD(P)H} \rightarrow 2\text{NO}_3^- + \text{NAD(P)}^+ + \text{H}^+$).³ In NOD reactions, including those observed with hemoglobins and myoglobins, an Fe(III)-superoxo species ($\text{Fe}^{\text{III}}(\text{O}_2^{\bullet-})$), which is generated in the reaction of Fe(II) + O_2 , reacts with NO to yield NO_3^- via formation of an Fe^{III}-PN intermediate.^{4,5} Here, a ferryl species ($\text{Fe}^{\text{IV}}(\text{O})$) is proposed to be formed via homolytic O–O bond cleavage of the Fe^{III}-PN species; Groves et al. only very recently provided time-resolved spectrophotometric evidence for the formation of such a ferryl species in the reaction of myoglobin with PN.⁶ However, a heme-PN moiety has not been detected due to its expected short lifetime and rapid recombination with NO_2 in a $[\text{Fe}^{\text{IV}}=\text{O} \cdot \text{NO}_2]$ cage to give a NO_3^- product. Thus, the study of metal-superoxo

intermediates with NO is of great interest with regard to the investigation of reaction pathways or undetected intermediate reactivity, such as in the possible escape of a bound PN or NO_2 molecule.⁷

Recently, *N*-tetramethylated cyclam⁸ (TMC)-chelated redox-active first-row transition metal complexes and their peroxo (O_2^{2-}) and superoxo ($\text{O}_2^{\bullet-}$) derivatives have been systematically synthesized and investigated in various oxidation reactions.^{9–12} In the cases of Ni and Cr complexes with 14-TMC and 12-TMC ligands,¹³ the TMC ring size was found to alter the structure of the resulting $[\text{M}(n\text{-TMC})(\text{O}_2)]^{n+}$ complexes; the larger ring size ligand (e.g., 14-TMC) forms metal-superoxo complexes (e.g., $\text{Ni}^{\text{II}}\text{-O}_2^{\bullet-}$ ^{10b} and $\text{Cr}^{\text{III}}\text{-O}_2^{\bullet-}$ ¹¹), whereas the smaller ring size 12-TMC chelate forms metal-peroxo complexes (e.g., $\text{Ni}^{\text{III}}\text{-O}_2^{2-}$ ^{10b} and $\text{Cr}^{\text{IV}}\text{-O}_2^{2-}$ ¹²). In addition, we recently reported the NOD reactivity of the Cr^{IV}-peroxo complex: this species reacted with NO to give a Cr(III)-nitrate product, $[\text{Cr}^{\text{III}}(12\text{-TMC})(\text{NO}_3)(\text{Cl})]^+$, but no intermediates such as Cr-PN or Cr-oxo species were detected.¹²

We herein report the reactions of the end-on Cr^{III}- $\text{O}_2^{\bullet-}$ complex bearing the 14-TMC ligand, $[\text{Cr}^{\text{III}}(14\text{-TMC})(\text{O}_2)(\text{Cl})]^+$ (**1**), with NO. Reaction of complex **1** with 1 equiv of NO generates a stable Cr(IV)-oxo species, $[\text{Cr}^{\text{IV}}(14\text{-TMC})(\text{O})(\text{Cl})]^+$ (**3**), via the formation of a presumed Cr^{III}-PN intermediate, $[\text{Cr}^{\text{III}}(14\text{-TMC})(\text{OON}=\text{O})(\text{Cl})]^+$ (**2**) (Scheme 1, reactions a and b), unlike the NO reaction of a Cr^{IV}- O_2^{2-}

Scheme 1



Received: June 12, 2013

Published: September 25, 2013

complex bearing 12-TMC.¹² To the best of our knowledge, this study presents the first strong evidence for the formation of a high-valent metal-oxo complex in the reaction of a metal-superoxo species and NO. Further, **3** does not lead to a NO₃⁻-containing product with NO₂ addition, but it does react with NO to give a Cr(III)-nitrito complex, [Cr^{III}(14-TMC)(NO₂)(Cl)]⁺ (**4**) (Scheme 1, reaction c). Thus, we were able to follow all the reaction pathways of metal–oxygen intermediates with NO, employing isolated or spectroscopically well-characterized Cr complexes.

The starting chromium complex, [Cr^{II}(14-TMC)(Cl)]Cl, was synthesized according to literature methods, and the Cr^{III}-O₂^{•-} complex (**1**, 2 mM) was prepared by bubbling O₂ for 30 s in an CH₃CN solution containing the starting complex at -40 °C, giving a dark red color.¹¹ After the reaction solution was purged with Ar for 30 min at -40 °C, 1 equiv of NO¹⁴ was added, and the mixture was stirred for 20 min (see Supporting Information (SI), Figure S1, for a schematic diagram showing the NO purification setup), whereupon the color of the solution changed from red to yellowish green (see Figure 1 for the UV/vis spectral changes). In

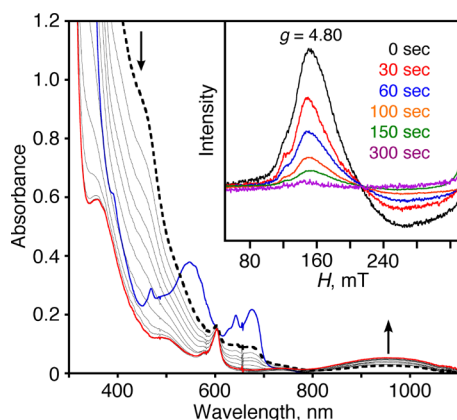


Figure 1. Changes in the UV/vis spectrum **1** (2 mM) upon addition of 1 equiv of NO in CH₃CN at -40 °C under Ar. The initial blue solid line spectrum (**1**) changed immediately to the black dashed line spectrum (**2**) upon addition of NO, followed by the conversion to the red solid line spectrum (**3**) over 15 min. Inset: time-dependent EPR spectra of Cr^{III}-PN intermediate (**2**) in CH₃CN at 5 K. **1** and NO were mixed in CH₃CN at -40 °C under Ar, and EPR spectra were obtained from such frozen solutions as a function of time (0, 30, 60, 100, 150, and 300 s).

this experiment, the spectrum of **1** changed from the blue solid line to the black dashed line immediately upon addition of NO, followed by conversion of this intermediate (**2**) to the Cr^{IV}-oxo species (**3**, red line) with $\lambda_{\max} = 603$ nm (80 M⁻¹ cm⁻¹) over 15 min (Figure 1). This final absorption spectrum is consistent with our previous report on the Cr^{IV}-oxo complex with 14-TMC,¹¹ and the conversion of **1** to **3** turned out to be quantitative. A resonance Raman spectrum of **3** was collected using 407-nm excitation in CH₃CN at -20 °C (Figure S2). The peak observed at 874 cm⁻¹ is comparable to the Cr–O frequency (873 cm⁻¹) of the previously reported [Cr^{IV}(14-TMC)(O)(Cl)]⁺ complex.¹¹ The electrospray ionization mass spectrum (ESI-MS) of **3** also supports the generation of Cr^{IV}-oxo species; the observed peak cluster centered at *m/z* 359.3 can be assigned to a Cr^{IV}-oxo complex formulated as [Cr^{IV}(14-TMC)(O)(Cl)]⁺ (calcd *m/z* 359.2) (Figure S3). An electron paramagnetic resonance (EPR) spectrum obtained for **3** (1 mM) in CH₃CN at 5 K was silent, consistent with the expected oxidation state of Cr^{IV} in **3**. Based on the spectroscopic characterization of **3**, we were able to

conclude unambiguously that a high-valent Cr^{IV}-oxo species was formed in the reaction of this Cr^{III}-O₂^{•-} complex and NO.

A proposed mechanism for the generation of a Cr^{IV}-oxo species (**3**) in the reaction of Cr^{III}-O₂^{•-} (**1**) and NO is depicted in Scheme 1. According to widely accepted discussions on the reaction mechanism of Fe^{III}-O₂^{•-} species with NO,^{2–6} the first step must be a radical-coupling reaction between **1** and NO to generate the Cr^{III}-PN intermediate, [Cr^{III}(14-TMC)(OON=O)(Cl)]⁺ (**2**) (Scheme 1, reaction a). This species gives rise to **3** and NO₂ via O–O bond homolysis of the PN ligand (Scheme 1, reaction b). The Cr^{IV}-oxo species generated does not react further with the NO₂ produced simultaneously, unlike the case for NOD reactions,^{3–6} and it maintains its metal-oxo structure under the reaction conditions.

We then attempted to characterize the presumed Cr^{III}-PN intermediate (**2**) and elucidate the mechanism of its conversion to the Cr^{IV}-oxo species (**3**) (Scheme 1, reaction b). First, the UV/vis spectrum shown as a black dashed line in Figure 1 likely represents that of **2**. Notably, the dashed line spectrum and the following changes shown in Figure 1 were not observed when the reaction was carried out at higher temperatures (e.g., 0 °C). For this latter experiment, the spectrum changed instantly from the blue solid line (**1**) to the red line (**3**) without showing any intermediate spectra, implying that the stability of **2** depends on the reaction temperature and **2** is detectable only at low temperature. We also found via EPR measurements that the intermediate species (i.e., the black dashed line in Figure 1) exhibited a signal assignable to a d³ Cr(III) ion (*S* = 3/2) at 5 K (Figure S4a),¹⁵ while complexes **1** and **3** were EPR-silent. Moreover, time-dependent EPR measurements revealed the clear conversion of **2** to **3**: EPR spectra in CH₃CN at 5 K obtained by freezing solutions of the **1** + NO reaction mixture as a function of time (0–300 s) indicated that the signal intensity decreased as time passed, leading from EPR-active **2** to EPR-silent **3** (Figure 1, inset). Thus, the Cr(III) EPR signal detected for **2** supports the generation of a Cr^{III}-PN species, which decomposes to the EPR-silent species **3**.¹⁶ As reported previously, the lifetimes of metal-peroxynitrite species are very short for species generated near room temperature.¹⁷ A striking recent success is a Co^{III}-PN porphyrinate complex, yet still generated under cryogenic conditions, but thoroughly characterized by using IR spectroscopy and isotope labeling experiments along with density functional theory (DFT) calculations.¹⁸

DFT calculations were also performed to further support our suppositions concerning the intermediacy of Cr^{III}-PN complex **2**. Complex **1** is an *S* = 1 state species,^{9a,11b} but upon addition of the NO spin (up or down), the whole system can reside in two energetically degenerate states, *S* = 1/2 or 3/2. The calculations reveal that the *S* = 1/2 state features a concerted high-energy barrier for the current reaction (Figure 2), and it is therefore not discussed further.¹⁹ The *S* = 3/2 state reaction pathway is shown to be able to proceed in two low-energy steps. The first step occurs over a low barrier of 1.7 kcal/mol, such that a very fast reaction of **1** with NO would occur, and alternative reactions are unlikely. Moreover, the product is the stable O-bound PN species **2** at -10.8 kcal/mol (Figure S5). The second step occurs over a barrier of 20.1 kcal/mol to form the Cr^{IV}-oxo complex **3**. This barrier is somewhat high, but it is likely overestimated.²⁰ All in all, the interpretation of the calculations strongly supports that the formation of the *S* = 3/2 species **2** is likely, and its transformation to **3** is quite possible.

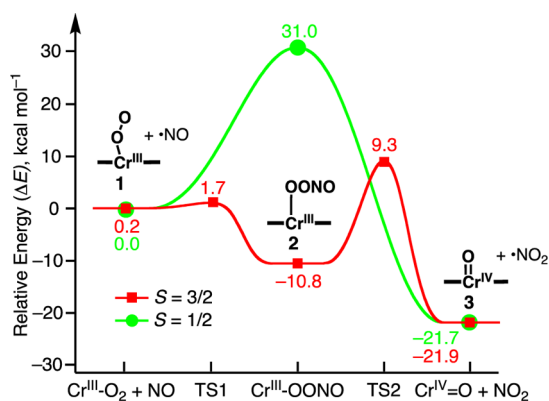
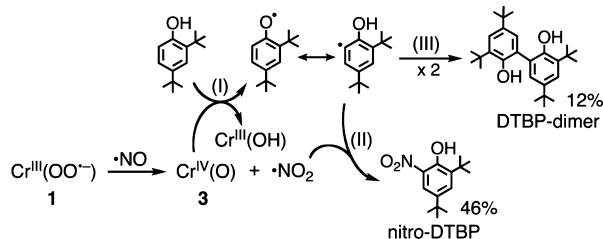


Figure 2. DFT-calculated pathways for the reaction of $[\text{Cr}^{\text{III}}(14\text{-TMC})(\text{O}_2)(\text{Cl})]^+$ (**1**) with NO. The low-energy two-step pathway giving PN complex **2** and then $\text{Cr}^{\text{IV}}=\text{O}$ species **3** occurs on the $S = 3/2$ surface (red, ■), while the $S = 1/2$ surface (green, ●) exhibits a concerted pathway that does not feature a (stable) peroxyxynitrite intermediate (**2**).

We sought more support for our mechanistic proposal, including the formation of **3** from **2** with the liberation of NO_2 . In this regard, we carried out trapping experiments using 2,4-di-*tert*-butylphenol (DTBP) to obtain evidence that NO_2 is produced concomitantly with the $\text{Cr}^{\text{IV}}=\text{O}$ formation (Scheme 1, reaction b).²² After the generation of **3** as discussed above, 1 equiv of DTBP was added to the resulting solution, which was then stirred for 20 min under Ar, while the reaction's UV/vis spectral changes were monitored (see Figure S6). ESI-MS analysis of the resulting solution revealed the presence of a Cr^{III} -hydroxo species at m/z 360.2 ($[\text{Cr}^{\text{III}}(14\text{-TMC})(\text{OH})(\text{Cl})]^+$, calcd m/z 360.3; Figure S6). Further product analysis was performed using GC and ^1H NMR spectroscopic measurements. Nitrated DTBP (2,4-di-*tert*-butyl-6-nitrophenol, nitro-DTBP) and oxidatively dimerized DTBP (2,2'-dihydroxy-3,3',5,5'-tetra-*tert*-butylbiphenol, DTBP-dimer) were produced in 46% and 12% yields, respectively (see SI for experimental details). The results can be readily explained as follows: First, H-atom abstraction reaction of DTBP by **3** gives a phenoxyl radical and a Cr^{III} -hydroxo complex (Scheme 2,

Scheme 2



reaction I). The phenoxyl radical traps gaseous NO_2 to give nitro-DTBP (Scheme 2, reaction II) or dimerizes to give DTBP-dimer (Scheme 2, reaction III). Thus, the fact that we successfully trapped and recovered NO_2 in good yield strongly supports the proposed reaction mechanism involving the formation of a $\text{Cr}^{\text{IV}}=\text{O}$ complex and NO_2 via homolytic O–O bond cleavage of a Cr^{III} -PN intermediate (Scheme 1, reaction b).

In heme and non-heme systems, the reaction of a ferryl species and NO has been of great interest in terms, for example, of the inhibition of cytochrome *bd* oxidase reactivity.²³ Here, a ferryl heme species reacts with NO to generate a ferric species and

nitrite ($\text{Fe}^{\text{III}} + \text{NO}_2^-$),^{23,24} while a ferryl non-heme complex ($[\text{Fe}^{\text{IV}}(14\text{-TMC})(\text{O})(\text{OAc})]^+$) with added NO produces a ferrous species and nitrite ($\text{Fe}^{\text{II}} + \text{NO}_2^-$).²⁵ The reactions of other metal-oxo complexes and NO have also been discussed.²⁶ Since we did not observe NO_3^- formation via a coupling between the $\text{Cr}^{\text{IV}}=\text{O}$ complex **3** and NO_2 (*vide supra*) and the formation of a Cr^{III} -nitrito complex, $[\text{Cr}^{\text{III}}(14\text{-TMC})(\text{NO}_2)(\text{Cl})]^+$ (**4**), was observed when an excess amount of NO was used in the reaction of $\text{Cr}^{\text{III}}-\text{O}_2^{\bullet-}$ complex **1**, we decided to check if **3** could react with NO, not with NO_2 , to form **4** (Scheme 1, reaction c). Indeed, this is the case. After **3** was generated as described above, the solution was degassed by Ar bubbling to remove NO_2 (*vide supra*), and then excess NO was added over the top of the solution at -40°C . The UV/vis spectral changes upon addition of NO and the ESI-MS of the resulting solution are depicted in Figure 3; the

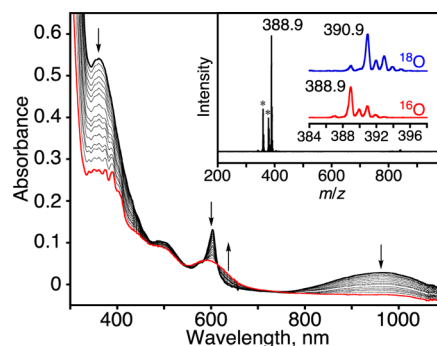


Figure 3. Changes in the UV/vis spectrum of **3** (black line) upon addition of NO (10 cm^3) into the headspace above a solution of **3** in CH_3CN at -40°C under Ar. Inset: ESI-MS spectrum of $[\text{Cr}^{\text{III}}(14\text{-TMC})(\text{NO}_2)(\text{Cl})]^+$ (**4**) (calcd m/z 389.1) and isotope distribution patterns for $4\text{-}^{16}\text{O}$ (red) and $4\text{-}^{18}\text{O}$ (blue). The peaks at m/z 359.1 and 378.1 marked with asterisks are assigned to $[\text{Cr}^{\text{IV}}(14\text{-TMC})(\text{O})(\text{Cl})]^+$ (calcd m/z 359.2) and $[\text{Cr}^{\text{III}}(14\text{-TMC})(\text{Cl}_2)]^+$ (calcd m/z 378.1), respectively.

characteristic absorption band of **3** at 603 nm disappeared gradually over 5 min, and a molecular ion peak corresponding to **4** appeared at m/z 388.9. When **1** was prepared with isotopically labeled $^{18}\text{O}_2$ and used in the subsequent reaction with NO, a peak corresponding to $[\text{Cr}^{\text{III}}(14\text{-TMC})(\text{N}^{18}\text{O}^{16}\text{O})(\text{Cl})]^+$ (calcd m/z 391.2) was found at m/z 390.9 (Figure 3, inset). The 2-mass-unit shift observed upon substitution of ^{16}O with ^{18}O indicates that **4** has one ^{18}O oxygen (out of two) in it and its origin is the $\text{Cr}^{\text{III}}-\text{O}_2^{\bullet-}$ complex **1** via $\text{Cr}^{\text{IV}}=\text{O}$ species **3** (Scheme 1, reaction c). Additionally, an EPR spectrum of **4** in CH_3CN at 5 K showed a signal assigned to a d^3 Cr(III) ion ($S = 3/2$)¹⁵ (Figure S3b). Based on the results presented above, we conclude that one-electron reduction of Cr occurs through the reaction between **3** and NO, resulting in the formation of $[\text{Cr}^{\text{III}}(14\text{-TMC})(\text{NO}_2)(\text{Cl})]^+$ (**4**; see Figure S6).

In summary, we have demonstrated the generation of a stable $\text{Cr}(\text{IV})=\text{O}$ species (**3**) in the reaction of a $\text{Cr}(\text{III})$ -superoxo complex (**1**) and nitric oxide. This is the first clear observation of metal-oxo species generation in the reaction of a metal-superoxo complex and NO via metal-peroxyxynitrite formation and subsequent homolytic O–O bond cleavage. This opens the way to utilize such an approach to generate biochemical or synthetic higher-valent metal-oxo species. Interestingly, the $\text{Cr}(\text{IV})=\text{O}$ species did not show any reactivity toward NO_2 , unlike NOD reactions, but it readily reacted with NO to form a $\text{Cr}(\text{III})$ -nitrito complex (**4**). In addition, we have shown that the

ring size of the TMC ligand has a significant effect not only on the determination of metal-O₂ structures but also on the reactivity of the resulting metal-oxo complexes toward NO and NO₂.

■ ASSOCIATED CONTENT

■ Supporting Information

Experimental details, purification of NO, trapping experiments, spectroscopic and kinetic data, and DFT calculations. This material is available free of charge via the Internet at <http://pubs.acs.org>.

■ AUTHOR INFORMATION

Corresponding Authors

karlin@jhu.edu

wwnam@ewha.ac.kr

Notes

The authors declare no competing financial interest.

■ ACKNOWLEDGMENTS

The authors gratefully acknowledge research support of this work by the NRF of Korea through CRI (2-2012-1794-001-1 to W.N.) and GRL (2010-00353 to W.N.) and the U.S. National Institutes of Health (K.D.K.).

■ REFERENCES

- (1) (a) Ignarro, J. E. *Nitric Oxide, Biology and Pathobiology*; Academic Press: San Diego, CA, 2000. (b) Wasser, I. M.; de Vries, S.; Moënne-Loccoz, P.; Schröder, I.; Karlin, K. D. *Chem. Rev.* **2002**, *102*, 1201. (c) Möller, J. K. S.; Skibsted, L. H. *Chem. Rev.* **2002**, *102*, 1167. (d) Richter-Addo, G. B.; Legzdins, P.; Burstyn, J. *Chem. Rev.* **2002**, *102*, 857. (e) Toledo, J. C., Jr.; Augusto, O. *Chem. Res. Toxicol.* **2012**, *25*, 975.
- (2) (a) Ford, P. C.; Fernandez, B. O.; Lim, M. D. *Chem. Rev.* **2005**, *105*, 2439. (b) Schopfer, M. P.; Wang, J.; Karlin, K. D. *Inorg. Chem.* **2010**, *49*, 6267. (c) Fry, N. L.; Mascharak, P. K. *Acc. Chem. Res.* **2011**, *44*, 289. (d) Heilman, B. J.; St. John, J.; Oliver, S. R. J.; Mascharak, P. K. *J. Am. Chem. Soc.* **2012**, *134*, 11573. (e) Berto, T. C.; Speelman, A. L.; Zheng, S.; Lehnert, N. *Coord. Chem. Rev.* **2013**, *257*, 244. (f) Xu, N.; Goodrich, L. E.; Lehnert, N.; Powell, D. R.; Richter-Addo, G. B. *Angew. Chem., Int. Ed.* **2013**, *52*, 3896. (g) Martirosyan, G. G.; Kurtikyan, T. S.; Azizyan, A. S.; Iretskii, A. V.; Ford, P. C. *J. Inorg. Biochem.* **2013**, *121*, 129.
- (3) (a) Doyle, M. P.; Hoekstra, J. W. *J. Inorg. Biochem.* **1981**, *14*, 351. (b) Eich, R. F.; Li, T.; Lemon, D. D.; Doherty, D. H.; Curry, S. R.; Aitken, J. F.; Mathews, A. J.; Johnson, K. A.; Smith, R. D.; Phillips, G. N., Jr.; Olsen, J. S. *Biochemistry* **1996**, *35*, 6976. (c) Gardner, P. R.; Gardner, A. M.; Martin, L. A.; Salzman, A. L. *Proc. Natl. Acad. Sci. U.S.A.* **1998**, *95*, 10378.
- (4) (a) Ouellet, H.; Ouellet, Y.; Richard, C.; Labarre, M.; Wittenberg, B.; Wittenberg, J.; Guertin, M. *Proc. Natl. Acad. Sci. U.S.A.* **2002**, *99*, 5902. (b) Gardner, P. R. *J. Inorg. Biochem.* **2005**, *99*, 247.
- (5) (a) Mehl, M.; Daiber, A.; Herold, S.; Shoun, H.; Ullrich, V. *Nitric Oxide* **1999**, *3*, 142. (b) Ferrer-Sueta, G.; Radi, R. *ACS Chem. Biol.* **2009**, *4*, 161. (c) Perrin, D.; Koppenol, W. H. *Arch. Biochem. Biophys.* **2000**, *377*, 266.
- (6) Su, J.; Groves, J. T. *Inorg. Chem.* **2010**, *49*, 6317.
- (7) (a) Schopfer, M. P.; Mondal, B.; Lee, D.-H.; Narducci Sarjeant, A. A.; Karlin, K. D. *J. Am. Chem. Soc.* **2009**, *131*, 11304. (b) Park, G. Y.; Deepalatha, S.; Pui, S. C.; Lee, D.-H.; Mondal, B.; Narducci Sarjeant, A. A.; del Rio, D.; Pau, M. Y. M.; Solomon, E. I.; Karlin, K. D. *J. Biol. Inorg. Chem.* **2009**, *14*, 1301. (c) Maiti, D.; Lee, D.-H.; Narducci Sarjeant, A. A.; Pau, M. Y. M.; Solomon, E. I.; Gaoutchenova, K.; Sundermeyer, J.; Karlin, K. D. *J. Am. Chem. Soc.* **2008**, *130*, 6700. (d) Herold, S.; Koppenol, W. H. *Coord. Chem. Rev.* **2005**, *249*, 499. (e) Pestovsky, O.; Bakac, A. *J. Am. Chem. Soc.* **2002**, *124*, 1698.
- (8) Barefield, E. K. *Coord. Chem. Rev.* **2010**, *254*, 1607.
- (9) (a) Cho, J.; Sarangi, R.; Nam, W. *Acc. Chem. Res.* **2012**, *45*, 1321. (b) Cho, J.; Jeon, S.; Wilson, S. A.; Liu, L. V.; Kang, E. A.; Braymer, J. J.;

Lim, M. H.; Hedman, B.; Hodgson, K. O.; Valentine, J. S.; Solomon, E. I.; Nam, W. *Nature* **2011**, *478*, 502.

(10) (a) Kieber-Emmons, M. T.; Annaraj, J.; Seo, M. S.; Van Heuvelen, K. M.; Tosha, T.; Kitagawa, T.; Brunold, T. C.; Nam, W.; Riordan, C. G. *J. Am. Chem. Soc.* **2006**, *128*, 14230. (b) Cho, J.; Sarangi, R.; Annaraj, J.; Kim, S. Y.; Kubo, M.; Ogura, T.; Solomon, E. I.; Nam, W. *Nature Chem.* **2009**, *1*, 568.

(11) (a) Cho, J.; Woo, J.; Nam, W. *J. Am. Chem. Soc.* **2010**, *132*, 5958. (b) Cho, J.; Woo, J.; Nam, W. *J. Am. Chem. Soc.* **2012**, *134*, 11112.

(12) Yokoyama, A.; Han, J. E.; Cho, J.; Kubo, M.; Ogura, T.; Siegler, M. A.; Karlin, K. D.; Nam, W. *J. Am. Chem. Soc.* **2012**, *134*, 15269.

(13) Abbreviations used: 12-TMC, 1,4,7,10-tetramethyl-1,4,7,10-tetraazacyclododecane; 14-TMC, 1,4,8,11-tetramethyl-1,4,8,11-tetraazacyclotetradecane.

(14) A NO-saturated solution was prepared under 1 atm at 298 K; the concentration of the NO in CH₃CN at 293 K was approximated to be 14 mM. For the published values for NO solubilities in organic solvents, see: Young, C. L. *Oxides of Nitrogen*; Solubility Data Series Vol. 8; International Union of Pure and Applied Chemistry: 1981. The purification of NO is described in the SI (experimental section and Figure S1).

(15) (a) Hempel, J. C.; Morgan, L. O.; Lewis, W. B. *Inorg. Chem.* **1970**, *9*, 2064. (b) Ueki, S.; Yamauchi, J. *Inorg. Chim. Acta* **2002**, *338*, 13.

(16) Characterization of the Cr^{III}-PN species **2** with ESI-MS in this case was unsuccessful due to its thermal instability. We note that there is no example of resonance Raman spectroscopic characterization of a metal-peroxynitrite complex, probably due to photodecay of the intermediate during measurements: Tran, N. G.; Kalyvas, H.; Skodje, K. M.; Hayashi, T.; Moënne-Loccoz, P.; Callan, P. E.; Shearer, J.; Kirschenbaum, L. J.; Kim, E. *J. Am. Chem. Soc.* **2011**, *133*, 1184.

(17) (a) Goldstein, S.; Lind, J.; Merényi, G. *Chem. Rev.* **2005**, *105*, 2457. (b) Yuki, E. T.; de Vries, S.; Moënne-Loccoz, P. *J. Am. Chem. Soc.* **2009**, *131*, 7234. (c) Kurtikyan, T. S.; Ford, P. C. *Chem. Commun.* **2010**, *46*, 8570.

(18) (a) Kurtikyan, T. S.; Eksuzyan, S. R.; Hayrapetyan, V. A.; Martirosyan, G. G.; Hovhannisyanyan, G. S.; Goodwin, J. A. *J. Am. Chem. Soc.* **2012**, *134*, 13861. (b) Wick, P. K.; Kissner, R.; Koppenol, W. H. *Helv. Chim. Acta* **2000**, *83*, 748.

(19) This would correspond to a reaction where the added NO abstracts an O-atom from the superoxo complex to directly produce NO₂.

(20) Inclusion of entropy and other correction factors, even though this process includes a formal error (see SI, DFT methods),²¹ gives an estimated barrier of 16.7 kcal/mol (see Table S1). In addition, dissociation entropy of NO₂ is expected to stabilize the products even more than what is calculated, thereby indirectly further lowering the transition state.

(21) Ho, J.; Klamt, A.; Coote, M. L. *J. Phys. Chem. A* **2010**, *114*, 13442.

(22) (a) Coombes, R. G.; Diggle, A. W. *Tetrahedron Lett.* **1993**, *34*, 8557. (b) Coombes, R. G.; Diggle, A. W. *Tetrahedron Lett.* **1994**, *35*, 6373. (c) Geletii, Y. V.; Patel, A. D.; Hill, C. L.; Casella, L.; Monzani, E. *React. Kinet. Catal. Lett.* **2002**, *77*, 277. (d) Ischiropoulos, H.; Zhu, L.; Chen, J.; Tsai, M.; Martin, J. C.; Smith, C. D.; Beckman, J. S. *Arch. Biochem. Biophys.* **1992**, *298*, 431. (e) Geletii, Y. V.; Bailey, A. J.; Boring, E. A.; Hill, C. L. *Chem. Commun.* **2001**, 1484.

(23) Borisov, V. B.; Forte, E.; Sarti, P.; Brunori, M.; Konstantinov, A. A.; Giuffrè, A. *FEBS Lett.* **2006**, *580*, 4823.

(24) Herold, S.; Rehmann, F.-J. *K. J. Biol. Inorg. Chem.* **2001**, *6*, 543.

(25) Owen, T. M.; Rohde, J.-U. *Inorg. Chem.* **2011**, *50*, 5283.

(26) (a) De Leo, M.; Ford, P. C. *J. Am. Chem. Soc.* **1999**, *121*, 1980. (b) Nemes, A.; Pestovsky, O.; Bakac, A. *J. Am. Chem. Soc.* **2002**, *124*, 421. (c) Man, W.-L.; Lam, W. W. Y.; Ng, S.-M.; Tsang, W. Y. K.; Lau, T.-C. *Chem.—Eur. J.* **2012**, *18*, 138.